EPJ Photovoltaics **8**, 85504 (2017)
www.epj-pv.org
DOI: 10.1051/epjpv/2017005



# High absorption coefficients of the $CuSb(Se,Te)_2$ and $CuBi(S,Se)_2$ alloys enable high-efficient 100 nm thin-film photovoltaics

Rongzhen Chen[1,2] and Clas Persson[1,2,3,a]

[1] Department of Materials Science and Engineering, KTH Royal Institute of Technology, SE-100 44 Stockholm, Sweden
[2] Centre for Materials Science and Nanotechnology, University of Oslo, P.O. Box 1048 Blindern, 0316 Oslo, Norway
[3] Department of Physics, University of Oslo, P.O. Box 1048 Blindern, 0316 Oslo, Norway

Received: 29 January 2017 / Received in final form: 27 February 2017 / Accepted: 4 May 2017


**Abstract** We demonstrate that the band-gap energies $E_g$ of $CuSb(Se,Te)_2$ and $CuBi(S,Se)_2$ can be optimized for high energy conversion in very thin photovoltaic devices, and that the alloys then exhibit excellent optical properties, especially for tellurium rich $CuSb(Se_{1-x}Te_x)_2$. This is explained by multi-valley band structure with flat energy dispersions, mainly due to the localized character of the Sb/Bi $p$-like conduction band states. Still the effective electron mass is reasonable small: $m_c \approx 0.25m_0$ for $CuSbTe_2$. The absorption coefficient $\alpha(\omega)$ for $CuSb(Se_{1-x}Te_x)_2$ is at $\hbar\omega = E_g + 1$ eV as much as 5–7 times larger than $\alpha(\omega)$ for traditional thin-film absorber materials. Auger recombination does limit the efficiency if the carrier concentration becomes too high, and this effect needs to be suppressed. However with high absorptivity, the alloys can be utilized for extremely thin inorganic solar cells with the maximum efficiency $\eta_{max} \approx 25\%$ even for film thicknesses $d \approx 50{-}150$ nm, and the efficiency increases to ∼30% if the Auger effect is diminished.

## 1 Introduction

Chalcopyrite $Cu(In,Ga)Se_2$ (CIGS) has become a commercialized absorber for thin-film photovoltaics (PV), and laboratory devices has reached the solar conversion efficiency of $\eta = 22.6\%$ by the ZSW in Baden-Württemberg [1]. $Cu_2ZnSn(S,Se)_4$ (CZTSSe) has the last decade attracted much attention, and the material is considered as a promising emerging inorganic PV material. CZTSSe has not only earth-abundant and low-cost elements but, similar to CIGS, also tunable band-gap energy and large absorption coefficient. The maximum efficiency for CZTSSe based solar cell is today 12.6% by the IBM in New York [2]. However, the device efficiency together with the material usage and manufacturing costs of CIGS and CZTSSe technologies must be considered. The total world energy consumption is estimated to be double by the year of 2050 referring to the current level [3]. In order to meet these future needs, it is important to explore novel materials as well as to develop different types of solar energy technologies, especially for large scale PV production. Finding alternative absorber materials for low-cost PV technologies is an ongoing research. CIGS and CZTSSe devices are produced with the absorber thickness of typically $d \approx 1000$ nm. Devices with thinner films reduce the material usage as well as decrease the path for carrier collection, but thinner films imply less absorption of the sunlight and that effect reduces the conversion efficiency considerably as the absorptivity depends exponentially on the thickness. Therefore, developing "ultrathin" ($d < 100$ nm) inorganic PV devices requires also tailor-making new materials with higher absorption coefficients. One way to enable ultrathin devices is to utilize nanostructures, like light-scattering nanoparticles or quantum dots, but that involves additional growth processes. Instead, using traditional $p$-$n$ junction technologies, a higher capacity to absorb light is required. $Cu(Sb/Bi)(S/Se)_2$ compounds (i.e., $CuSbS_2$, $CuSbSe_2$, $CuBiS_2$, and $CuBiSe_2$) have been demonstrated to have much higher absorption coefficients than CIGS and CZTSSe alloys [4–10]. These Sb/Bi containing chalcostibites have fairly inexpensive and earth-abundant elements, and the materials are thus interesting for thin PV technologies. The compounds have indirect-gap energies, however the difference between indirect and direct band-gap energies is only 0.1–0.3 eV due

[a] e-mail: Rongzhen.Chen@gmail.com

to the rather flat lowest conduction band (CB) [4,5,11]. The experimental values of the band-gaps energies are ∼1.5 eV [12], ∼1.65 eV [13], and ∼1.09 eV [14] for $CuSbS_2$, $CuBiS_2$, and $CuSbSe_2$, respectively. No experimental gap is available for $CuBiSe_2$, but the calculated gap energy is ∼1.13 eV [4,11]. The conversion efficiency is around 3% for devices based on $CuSbS_2$ or $CuSbSe_2$ [15,16], so further investigations of the materials are required as well as development of the devices.

In this work, the electronic and optical properties of $CuSb(Se_{1-x}Te_x)_2$ and $CuBi(S_{1-x}Se_x)_2$ for the alloy compositions $x = 0$, 0.25, 0.50, 0.75 and 1 are explored theoretically, using hybrid functional approach based on the density functional theory (DFT). The maximum conversion efficiency $\eta_{max}$ is calculated with the Shockley-Queisser (SQ) model, using the DFT absorption coefficient $\alpha(\omega)$ and considering different thicknesses $d$ of the absorber films. The calculations reveal that all considered compounds have indirect gaps, and the fundamental gap energies are between 0.9 and 1.3 eV. By alloying the gap energies can be tuned in for optimized device efficiency. The lowest CBs are rather flat with a large DOS at the CB edge, especially for the $CuSb(Se,Te)_2$ alloys, and the DOS is large also near the valence band (VB) edge. Still, however, the effective electron masses are relatively small for both $CuSbTe_2$ and $CuBiSe_2$. Due to the flat energy dispersion, the absorption efficiencies are much higher in these alloys compared with those of CIGS and GaAs, especially for photon energies in the energy region $E_g$ to $E_g + 1$ eV; this region is of special importance for the efficiency in thin film PV technologies. Moreover, we find that the absorption for $CuSb(Se_{1-x}Te_x)_2$ with $x = 0.50{-}0.75$ is slightly higher than for the other alloys. These tellurium containing alloys have also suitable relation between the direct $E_g^d$ and the fundamental indirect $E_g$ band gaps, implying that these alloy compositions will have highest maximum conversion efficiency of the considered alloys. For these indirect-gap materials we find that the Auger effect plays an important role, where small variations in the intrinsic carrier concentration easily can change the efficiency by (2–4)%. Due to the Auger effect the $CuSb(Se,Te)_2$ and $CuBi(S,Se)_2$ alloys have some 5% smaller efficiency compared to direct-gap materials for thick films ($d > 1000$ nm). However, for very thin films ($d < 400$ nm) the $CuSb(Se,Te)_2$ and $CuBi(S,Se)_2$ alloys have significantly higher efficiency than the traditional absorbers. The $CuSb(Se,Te)_2$ alloys remain a maximum efficiency of $\eta_{max} \approx (23{-}28)\%$ for $d = 50{-}200$ nm. Thus, $CuSb(Se_{1-x}Te_x)_2$ and $CuBi(S_{1-x}Se_x)_2$ can be alternative compounds for ultrathin inorganic PV devices.

## 2 Computational methods

The calculations of the electronic structure and the optical properties were based on a ground-state DFT, employing the projector augmented wave basis set of the VASP package [17–19] and a hybrid functional (HSE06) [20]. The alloys ($x = 0$, 0.25, 0.50, 0.75, and 1) were modelled by small 16-atom unit cells, constructed from the ternary compounds with the space group *Pnma* (no. 62). We justify the small cells of the alloys by the more accurate HSE06 calculation of the optical properties regarding band dispersion and the **k**-space integration. The atomic positions and the lattice constants were relaxed with the quasi-Newton algorithm until a maximum force of 10 meV/Å of each atom was reached. The local, atomic- and angular-resolved DOS (LDOS) was obtained from the modified tetrahedron integration method with a Γ-centered $5 \times 8 \times 2$ **k**-mesh in the irreducible Brillouin zone. We excluded the spin orbit coupling (SOC) because we have found that there no degeneracies at the band edges that can be split by the SOC. In addition, SOC narrows the band-gap energy by only 0.1–0.2 eV, it does not change the materials from being indirect to direct, and it has only a moderate effect on the DOS.

The optical property of the alloys was analyzed by the means of the absorption coefficient $\alpha(\omega) = \omega c^{-1}(2|\varepsilon(\omega)| - 2\varepsilon_1(\omega))^{1/2}$, determined directly from the complex dielectric function $\varepsilon(\omega) = \varepsilon_1(\omega) + i\varepsilon_2(\omega)$, where $c$ is the speed of light. Here, the tensor $\varepsilon_2(\omega)$ with components $\alpha$ and $\beta$ (i.e., $\varepsilon_2^{\alpha\beta}(\omega)$) was calculated within the linear response of optical transition probability between occupied and unoccupied states $\varepsilon_2^{\alpha\beta}(\omega) = \lim_{\mathbf{q}\to 0} 4\pi^2 e^2 \Omega^{-1} \mathbf{q}^{-2} \sum_{c,v,\mathbf{k}} 2\omega_{\mathbf{k}} \cdot \delta(E_c(\mathbf{k}) - E_v(\mathbf{k}) - \hbar\omega) \times \langle u_c(\mathbf{k}+\mathbf{e}_\alpha \mathbf{q}) | u_v(\mathbf{k}) \rangle \langle u_c(\mathbf{k}+\mathbf{e}_\beta \mathbf{q}) | u_v(\mathbf{k}) \rangle^*$ (see Refs. [17–19] for details) and performing similar **k**-space integration as for the LDOS. Subsequently, $\varepsilon_1^{\alpha\beta}(\omega)$ was obtained via the Kramers-Kronig transformation with a broadening of 3 meV for the equidistant energy grid with step size of 2 meV up to the maximum energy of 65 eV. All DFT-based calculations were performed with HSE06 and with a cut-off energy of 420 eV. A large **k**-mesh can be important to describe details in the absorption coefficient [21,22]. However, from test calculations we have found that the effect is not crucial for the considered materials, and we use HSE06 (which avoids incorrect resonance across the underestimated gaps for local potentials [23,24]) and with the same **k**-mesh as for the calculations of the LDOS.

The maximum energy conversion efficiency $\eta_{max} = P_{max}/P_{in}$ of a single-junction cell was modelled within the SQ theory [25] assuming air mass 1.5 solar spectral irradiance $I_{sun}(\omega)$ and an absorptivity $A(\omega) = 1{-}\exp(-2{\cdot}\alpha(\omega){\cdot}d)$ in the absorber film with thickness $d$. $P_{in}$ is the Sun's total irradiance which is ∼1000 W/m$^2$. The maximum efficiency is reached for $P_{max} = J_{opt} \cdot V_{opt}$ where $J_{opt}$ and $V_{opt}$ are the current (per unit area) and the device voltage optimized for maximum power. Here, the current $J$ and the device voltage $V$ are balanced within the Shockley ideal diode equation [25–27]: $J = J_{sc} - J_r^0 \cdot q \cdot (\exp(qV/k_B T_c) - 1)$ where $q$ is the elementary charge, $k_B$ is the Boltzmann constant, and $T_c$ is the device temperature set to 300 K. The first term on the right hand side is the maximum short circuit current $J_{sc} = \hbar \cdot q \cdot \int A(\omega) \cdot I_{sun}(\omega) \partial\omega$. The second term is the thermal recombination current $J_r^0$ which can involve both radiative and non-radiative recombinations. Since we analyze the maximum efficiency of the materials, recombinations via defects are not considered in this study.

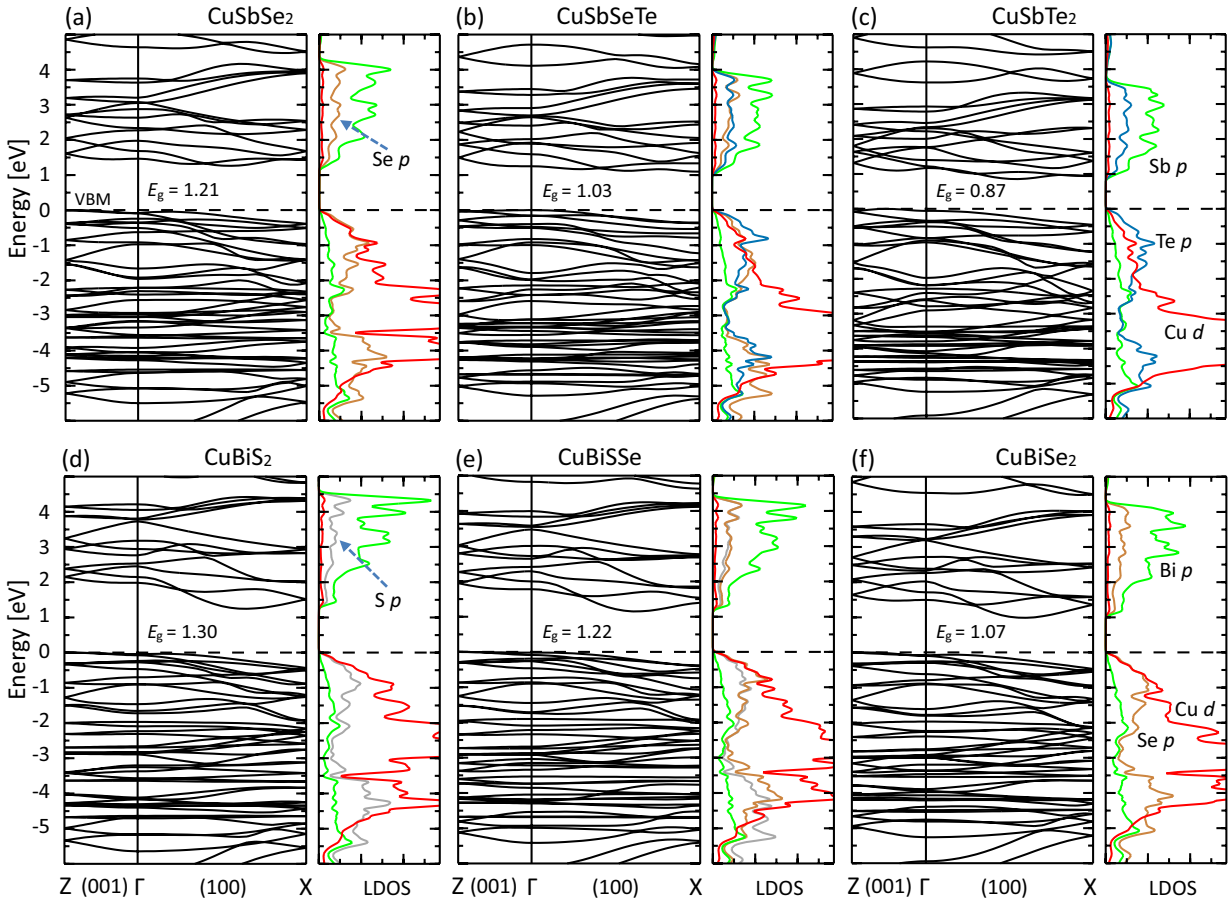


**Fig. 1.** Electronic band structure and LDOS of (a) $CuSbSe_2$, (b) CuSbSeTe, i.e., 50% alloying, (c) $CuSbTe_2$, (d) $CuBiS_2$, (e) CuBiSSe, 50% alloying, and (f) $CuBiSe_2$. The energy refers to the VBM (dashed lines). The atom- and angular momentum resolved density-of-states has been scaled with $1/(2l+1)$ for better visualization, and it is presented with a 0.20 eV Lorentzian broadening. One can notice the strong Sb/Bi $p$-like states in the lower energy region of the conduction bands.

## 3 Results

The crystal structure of the ternary compounds $CuSb(Se/Te)_2$ and $CuBi(S/Se)_2$ was fully relaxed with the hybrid functional. The lattice constants are, as normally for HSE06, slightly overestimated but in agreement within 4% with available experimental results: $a = 6.31$ Å, $b = 3.97$ Å, and $c = 14.65$ Å for $CuSbSe_2$, $a = 6.76$ Å, $b = 4.26$ Å, and $c = 15.45$ Å for $CuSbTe_2$, $a = 6.16$ Å, $b = 3.88$ Å, and $c = 14.20$ Å for $CuBiS_2$, and $a = 6.47$ Å, $b = 4.08$ Å, and $c = 14.64$ Å for $CuBiSe_2$. Relaxation of the $CuSb(Se,Te)_2$ and $CuBi(S,Se)_2$ quaternary alloys results in lattice parameters that follow, despite rather small unit cells, linearly within 0.5% with respect to the alloy composition $x$.

The electronic band structures of the $CuSb(Se,Te)_2$ and $CuBi(S,Se)_2$ alloys (Fig. 1) show strikingly flat energy dispersions for both the CBs and VBs. Overall, all compounds have similar band structure with indirect fundamental band gap $E_g$, where CB minima (CBM) tend to be along (100) direction while VB maxima (VBM) is along the (001) direction. The main difference between the compounds is the energy of this fundamental gap. $CuSbSe_2$ with the lighter group-V cation atom has gap energy $E_g = 1.21$ eV, which is 0.14 eV larger than for $CuBiSe_2$ with $E_g = 1.07$ eV. Also, the lighter group-VI anion Se atom in $CuSbSe_2$ yields a 0.34 eV larger gap compared with $CuSbTe_2$ with $E_g = 0.87$ eV. Similarly, the lighter S atom in $CuBiS_2$ ($E_g = 1.30$ eV) yields a 0.23 eV larger gap compared with $CuBiSe_2$; this energy difference is somewhat smaller than corresponding value of ∼0.5 eV for both $Cu_2ZnSn(S/Se)_4$ and $CuIn(S/Se)_2$ when comparing their group-VI anion atoms [28, 29]; heavier group-V atoms yields smaller energy difference. Thus, the heavier Bi atom yields the smallest variation of $E_g$ with respect to anion alloying. This is true also when comparing $CuSbSe_2$ with $CuSbS_2$ (not presented in this work). The band-gap energies for the alloys vary fairly linearly with alloy composition $x$ (Fig. 2); the small deviation from this is mainly due to cell sizes. In $CuSb(Se,Te)_2$ the direct gap at the Γ-point $E_g^\Gamma$ is about 0.4 eV larger than the indirect gap $E_g$, while the corresponding energy difference is about 0.7 eV in $CuBi(S,Se)_2$. In both the $CuSb(Se,Te)_2$ alloys and the $CuBi(S,Se)_2$ alloys, the direct $E_g^d$ gap energy is only ∼0.2 eV larger than the fundamental indirect $E_g$. This is a rather small energy difference, and that

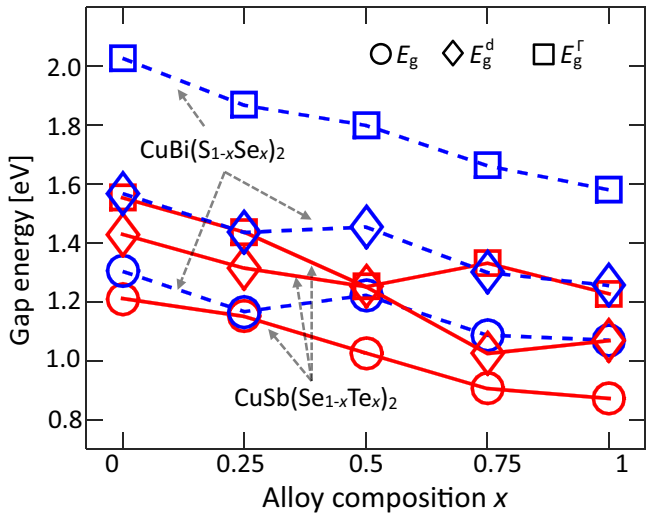


**Fig. 2.** Energies of the fundamental gap (circles), the direct gap (rhomboids), and the direct Γ-point gap (squares) for the $CuSb(Se,Te)_2$ alloy (red marks) and the $CuBi(S,Se)_2$ alloy (blue marks).

is important for enabling efficient photovoltaics. The direct gap governs the sunlight absorption and mainly also the radiative recombination, while the indirect gap governs the Auger non-radiative recombination. Therefore, optimizing the direct-gap energy by forming bands with small energy difference $\Delta_g = E_g - E_g^d$ is the route for tailor-making high-efficient PV materials with large joint DOS for energies just above $E_g^d$. The values of the band-gap energies are summarized in Table 1.

The error bar of the HSE06 band-gap energies is estimated to be typically about 0.1–0.2 eV. Our values agree well with earlier published calculated values for the $Cu(Sb/Bi)(S/Se)_2$ ternaries [4, 5, 11]. The experimental gap energies are not fully established, but the available room-temperature data [12–14] suggest that our theoretical values might be off by about 0.1 to 0.3 eV. However, since the direct-gap energies of these alloys are between about 1.0 and 1.6 eV and the optimized gap within the SQ theory is 1.2–1.4 eV, it is possible to find an alloy composition with the proper direct band-gap energy.

The LDOS in Figure 1 also demonstrates that all the compounds have comparable electronic structures (apart from the values of the gap energies). The CBs are dominated by relatively localized Sb/Bi $p$-like states and that generates a strong DOS close to the CB edges. This effect yields rather flat lowest CBs. Flat energy dispersion can imply large effective masses which are disadvantageous for the lifetime of the carries. However, the effective electron masses at the CBM are relatively small for these compounds, for instance: $m_x \approx 0.23m_0$, $m_y \approx 0.16m_0$, and $m_z \approx 0.40m_0$ for $CuSbTe_2$, and $m_x \approx 0.19m_0$, $m_y \approx 0.83m_0$, and $m_z \approx 0.50m_0$ for $CuBiSe_2$. These values are comparable to the corresponding calculated effective masses for CIGS ((0.08–0.13)$m_0$ [30]) and Si ($m_x = m_y \approx (0.19{-}0.22)m_0$; $m_z \approx (0.96{-}1.02)m_0$ [23, 24]), while considerably larger than that of GaAs ((0.06−0.09)$m_0$ [23, 24]). Interestingly, two of the mass components ($m_x$ and $m_z$) are similar for the two compounds, while the third compound (i.e., $m_y$) is significantly different. This may indicate that small variation in the crystal structure (e.g., strain, defects in resonance with the CBs) can easily change the band dispersion and thereby change the values of the effective masses, and this can thus be a way to optimize the material properties with respect to the effective masses. It is worth mentioning that the mass values are valued only in the vicinity of the CBM where the band is parabolic (at most 50 meV above CBM in these materials). However, even with small effective electron mass of $\sim 0.1m_0$ the quasi-Fermi level is only ∼20 meV above the CBM even for a high free electron concentration of $10^{17}$ cm$^{-3}$ [31]. Furthermore, the VBs in these Cu-based chalcostibites have the characteristic Cu-$d$–anion-$p$ hybridization that helps forming localized band structures near the valence band edges. Since the topmost VBs are flat, also the DOS near the valence-band edges are strong if one compare with the DOS of CIGS and CZTSSe. Thus, the $CuSb(Se,Te)_2$ and $CuBi(S,Se)_2$ compounds have flat CBs and VBs, and that is an advantage for a strong onset of the optical absorption.

Indeed, the absorption coefficients for these compounds (Fig. 3a) are significantly larger than corresponding calculated results for the traditional PV absorbers CIGS and GaAs; the figure shows $\alpha(\omega)$ on the energy scale $E = \hbar\omega - E_g^d$ in order to easier compare materials with different gap energies. This larger $\alpha(\omega)$ is especially notable in the energy region $E_g^d$ to $E_g^d + 1.5$ eV. For instance, at the photon energy $\hbar\omega = E_g^d + 1$ eV, the $CuSb(Se,Te)_2$ alloys have ∼7 times larger absorption coefficients than those of CIGS and GaAs. One notices also that the $CuSb(Se,Te)_2$ alloys have slightly better absorption than the $CuBi(S,Se)_2$ alloys, however considering also the proper band-gap energies (Fig. 2) both the CuSb- and CuBi-based alloys have sufficiently good optical properties for thin film applications. The high-frequency dielectric constant ($\varepsilon_\infty$; see Tab. 1) is rather high, above 10 for all compounds; this can be compared with our calculated value 10.0 for GaAs and 7.0 for CIGS. The $CuSb(Se,Te)_2$ alloys have higher values ($13.0 \leq \varepsilon_\infty \leq 17.2$) compared with the $CuBi(S,Se)_2$ alloys ($10.5 \leq \varepsilon_\infty \leq 12.7$), and as expected the dielectric constant increases with larger alloy composition $x$, as the band-gap energy decreases. The related refractive index is a material property that needs to be considered when designing device with these compounds.

From the absorption coefficients and the gap energies, the device efficiency for the absorber material with thickness $d$ is determined within the SQ theory; see previous section. The maximum energy conversion efficiency $\eta_{max}$ is modelled by the Shockley ideal diode equation, considering both radiative recombination and non-radiative Auger recombination: $J_r^0 = J_{rad}^0 + J_{aug}^0$. The radiative recombinations depend on the black-body spectrum of the device: $J_{rad}^0 = (2\pi \cdot c)^{-2} \cdot \int A(\omega)\omega^2/(\exp(\hbar\omega/k_B T_c) - 1)\partial\omega$. The Auger recombinations in a $p$-type absorber depends

**Table 1.** The fundamental ($E_g$), direct ($E_g^d$), and Γ-point ($E_g^\Gamma$) gap energies, as well as the high-frequency dielectric constant ($\varepsilon_\infty$); we present the average dielectric constant since the anisotropy is rather small. The maximum solar conversion efficiency ($\eta_{max}$) is presented for two film thicknesses ($d$), and it includes both radiative and Auger recombinations (values in parenthesis are results when the Auger effect is neglected).

| Compound | $x$ | Gap energies [eV] | | | | $\varepsilon_\infty$ | $\eta_{max}$ [%] | |
|---|---|---|---|---|---|---|---|---|
| | | $E_g$ | $E_g^d$ | $E_g^\Gamma$ | $E_g^{expt}$ | | $d = 200$ nm | 50 nm |
| $CuSb(Se_{1-x}Te_x)_2$ | 0.00 | 1.21 | 1.43 | 1.55 | 1.09[a], 1.2[b] | 13.0 | 25.1 (28.5) | 19.8 (22.4) |
| | 0.25 | 1.15 | 1.31 | 1.44 | | 13.9 | 26.1 (28.1) | 20.9 (22.4) |
| | 0.50 | 1.03 | 1.25 | 1.25 | | 15.5 | 26.2 (30.3) | 22.3 (25.6) |
| | 0.75 | 0.91 | 1.02 | 1.33 | | 17.2 | 28.3 (29.8) | 23.8 (25.0) |
| | 1.00 | 0.87 | 1.07 | 1.23 | | 17.2 | 24.7 (29.8) | 21.0 (25.2) |
| $CuBi(S_{1-x}Se_x)_2$ | 0.00 | 1.30 | 1.57 | 2.03 | 1.65[c] | 10.5 | 20.3 (24.1) | 15.1 (17.8) |
| | 0.25 | 1.17 | 1.44 | 1.87 | | 11.0 | 21.0 (25.5) | 15.5 (18.7) |
| | 0.50 | 1.22 | 1.45 | 1.80 | | 11.6 | 23.4 (27.0) | 18.2 (20.9) |
| | 0.75 | 1.09 | 1.30 | 1.66 | | 12.3 | 24.2 (28.2) | 19.0 (22.1) |
| | 1.00 | 1.07 | 1.26 | 1.58 | | 12.7 | 24.3 (27.4) | 19.1 (21.5) |

[a] Tang et al. [14]
[b] Colombara et al. [12]
[c] Pawar et al. [13]

mainly on the intrinsic free carrier concentrations $n_i$ and the acceptor concentration $N_A$: $J^0_{aug} = q \cdot C_a \cdot d \cdot n_i^2 \cdot N_A$ [26] where $C_a$ is the total ambipolar Auger coefficient. This coefficient is rather independent of material (typically $10^{-32}$–$10^{-30}$ cm$^6$/s and it is in the order of $10^{-31}$ for indirect transition in Si and Ge and GaAs [32–35]. We want to estimate the Auger effect using an approximate model that is material independent, and we therefore set $C_a = 10^{-31}$ cm$^6$/s for all considered materials. The acceptor concentration is set to $N_A = 10^{16}$ cm$^{-3}$ which is a normal doping concentration. The square of the intrinsic carrier concentration can be expressed as $n_i^2 = n_a^2 \cdot \exp(E_g/k_B T_c)$ where $n_a = 2 \cdot (m_a k_B T_c/(2\pi\hbar^2))^{3/2}$ with the effective DOS mass $m_a = [(\gamma_e^{2/3} m_e^{DOS}) \cdot (\gamma_h^{2/3} m_h^{DOS})]^{1/2}$ where $\gamma_e$ is the number of CBM and $m_e^{DOS}$ is the effective DOS mass of a single CB minimum (and corresponding for the holes in the VB maximum). Again, to construct a material independent expression, we set $m_a = 1m_0$, which is a good value for indirect material like for instance Si (with six equivalent CBM) and somewhat overestimated for Ge (with three equivalent CBM). The value is however much larger than for direct materials, like GaAs and CIGS, but since the Auger effect is much weaker for these materials, using $m_a = 1m_0$ also for these direct-gap materials does not affect the results in this work.

The maximum efficiency $\eta_{max}$ for different film thicknesses $d < 1000$ nm is displayed in Figure 3b. One observes the typical drop in the efficiency for $d < 500$ nm for the traditional, direct-gap materials CIGS and GaAs. For $d$ larger than ∼500 nm CIGS and GaAs has higher efficiency than the $CuSb(Se,Te)_2$ and $CuBi(S,Se)_2$ alloys. If the thickness increases to even further (i.e., $d \to \infty$) then $\eta_{max}$ will become independent of the absorption coefficient, and it will only depend on the gap energy with $\eta_{max} = 33\%$ for both CIGS and GaAs. Also the $CuSb(Se,Te)_2$ and $CuBi(S,Se)_2$ alloys would have had similar high efficiency if they were direct-gap materials (e.g., then $\eta_{max}$ would have been 34% for $CuSbTe_2$ and 33% for $CuBiSe_2$). However, as being indirect-gap materials the Auger effect decreases their efficiencies by about 3–5%. This decrease due to the non-radiative recombination effect is fairly constant with respect to thickness $d$, and therefore the Auger effect is less dominant for smaller thicknesses where instead the efficiency drop is due to the lower absorptivity. That is, for thin films with $d < 500$ nm, the absorption coefficient in the low photon-energy region ($E_g$ to about $E_g + 1$ eV) is the important material property for retaining a high efficiency. One notices clearly that the $CuSb(Se,Te_2)$ and $CuBi(S,Se_2)$ alloys keep their efficiencies when the film thickness narrows to some 10–200 nm. Here, $CuBiS_2$ has a too large gap energy ($E_g^d = 1.57$ eV), and its efficiency is significantly lower than the other alloy compounds, but the other compounds have efficiencies close to 25% down to 100 nm. Further, the excellent optical properties of the $CuSb(Se,Te)_2$ and $CuBi(S,Se)_2$ alloys yield remarkable high efficiency even for $d = 50-100$ nm, especially for the CuSb-based compounds. The maximum efficiency is presented in Table 1 for two specific film thicknesses. The $CuSb(Se_{1-x}Te_x)_2$ with $x \approx 0.5-0.75$ has the highest efficiency. For instance $\eta_{max} = 28\%$ for $d = 200$ nm and $\eta_{max} = 24\%$ for $d = 50$ nm for $x = 0.75$. The reason for high efficiency of this alloy (i.e., $CuSb(Se_{1-x}Te_x)_2$ with $x = 0.75$) is that the energy difference $\Delta_g = E_g - E_g^d$ is only 0.11 eV. Here, the smaller $\Delta_g$ for this alloy might be due to using too small unit cell, and further investigation is required before establishing a result. Nonetheless, it demonstrates the sensitivity of $\eta_{max}$ with respect to small variation in the band structure. Moreover, the overall results demonstrate that $CuSb(Se_{1-x}Te_x)_2$ and $CuBi(S_{1-x}Se_x)_2$ can be alternative compounds for "ultrathin" ($d < 100$ nm) inorganic photovoltaics based

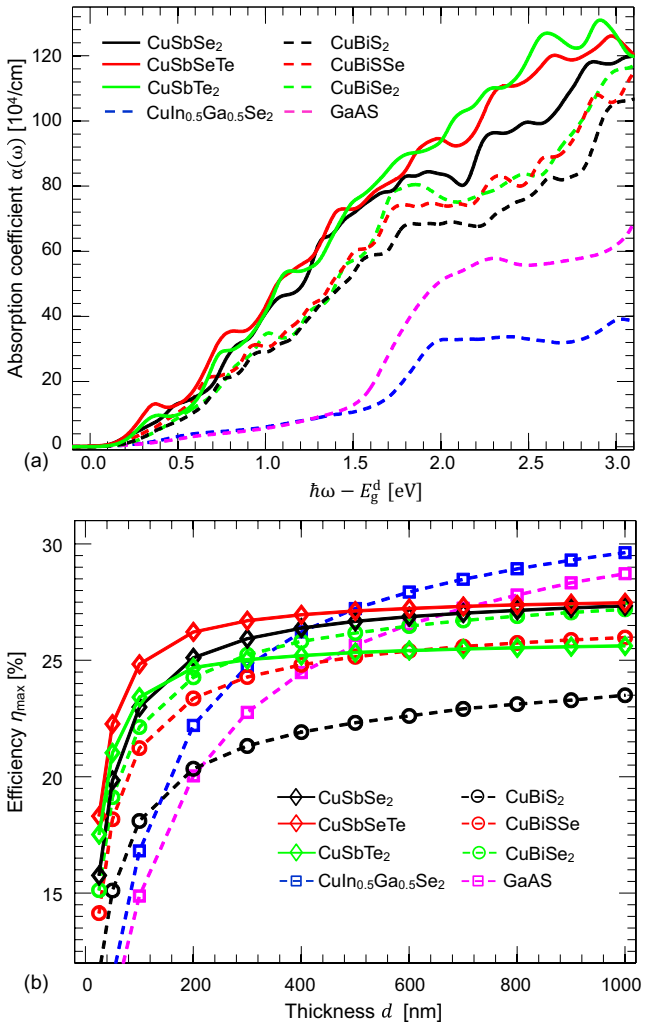


**Fig. 3.** (a) The absorption coefficients $\alpha(\omega)$ of $CuSbSe_2$, CuSbSeTe, $CuSbTe_2$, $CuBiS_2$, CuBiSSe, and $CuBiSe_2$ on the energy scale ($\hbar\omega - E_g^d$) and with a 0.30 eV Lorentzian broadening. These compounds exhibit much stronger near-gap-energy absorption compared to the traditional absorbers GaAs ($E_g$ ∼1.41 eV with HSE06) and CIGSe (50% alloying: $E_g$ ∼1.30 eV). (b) The corresponding maximum solar energy efficiency $\eta_{max}$ demonstrates high efficiency of $CuSb(Se,Te)_2$ and $CuBi(S,Se)_2$ alloys for very thin films of $d < 400$ nm (see also Tab. 1).

on traditional single $p$-$n$ junction technique. The advantage with such thin film absorber layer is the shorter path for the minority carriers. However many other material and device properties related to defects/doping and interface physics have to be controlled and optimized.

The values within brackets for $\eta_{max}$ in Table 1 show the efficiency if the Auger effect is neglected, demonstrating that this effect lowers the efficiency by ∼4%. One can significantly reduce the Auger recombination by decreasing the energy difference $\Delta_g$. If $\Delta_g$ goes from ∼0.2 eV to 0 eV, then the Auger effect is suppressed by the radiative recombination that determine the voltage drop. Then the maximum efficiency increases by 3–5% and reaching the efficiency very close to having no Auger effect. Alternatively, the Auger effect can be reduced by minimizing the carrier concentration since $J_{aug}^0 \propto n_i^2 N_A$. That can be achieved by using materials with large fundamental gap, but too large gap will be a disadvantage for the optical absorption. For $p$-type material, the efficiency is increased by ∼(1–2)% if the doping concentration decreases to $N_A = 10^{15}$ cm$^{-3}$. However, for intrinsic materials, the Auger model becomes $J_{aug}^0 \propto n_i^2 p$ [26] that depends even stronger on $\Delta_g$ and on the voltage drop, and this can result in even smaller efficiency. Alternatively, the carrier concentration can be decreased by smaller effective DOS masses. The employed effective DOS mass in this work is $m_a = 1m_0$ which is estimated to be somewhat too large, especially for $CuSbTe_2$. Instead, if using a smaller mass of $m_a = 0.4m_0$ (and with $\Delta_g \approx 0.2$ eV) the maximum efficiency of $CuSbTe_2$ increases by ∼1.5%. However, trying to optimize the electronic band structure to obtain even smaller DOS masses also means more dispersion of the band structure and thereby smaller absorption coefficient. Therefore, multi-valley engineering (with large joint DOS and large $\alpha(\omega)$) balanced with band-edge engineering for small effective masses (with low carrier concentration $n_i^2 \propto [(\gamma_e^{2/3} m_e^{DOS}) \cdot (\gamma_h^{2/3} m_h^{DOS})]^{3/2}$ and long lifetime) is the concept to tailor-make materials for even thinner PV devices. Here, better models that include non-parabolic energy dispersion together with better description for the absorption/recombination are required for more accurate describing the material behavior.

## 4 Conclusions

We have analyzed the electronic and optical properties of $CuSb(Se,Te)_2$ and $CuBi(S,Se)_2$ alloys for high-efficient thin-film PV technologies. The direct-gap energy can be tuned from ∼1.0 to 1.6 eV, and the fundamental indirect-gap energy is typically 0.2 eV smaller. The materials exhibit excellent optical properties, with absorption coefficients ∼6 times larger than for the traditional solar cell materials CIGS and GaAs in the low photon energy region. The main reason for the high absorption coefficients of these alloys is the strong Sb/Bi $p$-like character in the lower energy region of the CBs, forming flat multi-valley bands, and thereby yielding extraordinary strong absorption for photon with energies $E_g^d$ to $E_g^d + 1$ eV. Interestingly, even though the lowest CBs are flat, the corresponding effective electron masses of the CBM are reasonable small for both $CuSbTe_2$ (DOS mass is $m_e^{DOS} \approx 0.25m_0$ for a single CB minimum) and $CuBiSe_2$ ($m_e^{DOS} \approx 0.43m_0$). These DOS masses are heavier than for GaAs ($\sim 0.07m_0$), but using thinner absorber layers can compensate the larger masses.

For these indirect-gap materials we find that the Auger effect plays an important role. Small variations in the intrinsic carrier concentration can easily change the efficiency by ∼3%. Due to the Auger effect the $CuSb(Se,Te)_2$ and $CuBi(S,Se)_2$ alloys have some 4% smaller efficiency compared to direct-gap materials for relatively thick film

($d > 1000$ nm). The affect due to the Auger effect depends on the balance between the diode's voltage drop and the free carrier concentration. If the electron DOS mass is decreased from $1.0m_0$ to $0.4m_0$, then the intrinsic carrier concentration decreases by a factor of 2 and the efficiency increases by about 1.5%. Moreover, if the energy difference between the indirect and direct-gap energies goes to zero, then the Auger effect is negligible and the efficiency is increased by (3–5)%. Also Yu et al. [36] discuss this relation for indirect versus direct-gap, using the SQ model, though with a slightly different model for the Auger effect. Thus, the concept to optimize the device efficiency relies on creating materials with flat multi-valley band edges with direct energy gaps, where the carrier channels have high energy dispersions (i.e., small effective masses). Nonetheless, since the Auger effect is less sensitive to the film thickness, while the absorptivity depends strongly on the absorption coefficient for $d < 500$ nm, the $CuSb(Se,Te)_2$ and $CuBi(S,Se)_2$ alloys have significantly higher efficiency than the traditional absorbers for thinner film thicknesses. The $CuSb(Se,Te)_2$ with composition $x \approx 0.5{-}0.75$ has the largest absorption coefficient ($\alpha(\omega) \approx 1 \times 10^5$/cm already for the photon energy $\hbar\omega = E_g + 0.4$ eV) and proper gap energies $E_g^d = 1.02{-}1.25$ eV and $E_g = 0.91{-}1.03$ eV, and this compound exhibits highest efficiency for thin film thicknesses of $d < 400$ nm. The tellurium rich alloys remain an efficiency of $\eta_{max} \approx (25{-}27)\%$ when film thickness decreases to $d = 100$ nm. Including the exciton effect in the calculation can improve the efficiency further by a stronger absorption coefficient, though in bulk materials the effect is expected to be weaker at operating temperature.

Altogether, due to the outstanding optical properties we believe that $CuSb(Se_{1-x}Te_x)_2$ and $CuBi(S_{1-x}Se_x)_2$ can be alternative compounds for "ultrathin" ($d <$ 100 nm) inorganic photovoltaics. However, concern regarding material quality and modifications in the band dispersion is needed in order to minimize the non-radiative recombination. That is, to tailor-make materials for very thin, inorganic PV technologies one shall consider (*i*) an optimized band-gap energy for the specific film thickness; (*ii*) multi-valley band edges; and (*iii*) rather flat energy dispersions to achieve high absorption coefficient for the low photon energies $\hbar\omega = E_g$ to $E_g + 0.5$ eV. However, (*iv*) the band structure shall have direct fundamental gap to avoid Auger recombinations; thus both CBM and VBM shall then be located at the same **k**-point but away from the Γ-point. (*v*) Small DOS electron and hole masses reduce the intrinsic carrier concentration, which in turn reduces the Auger effect. Preferable, the material (*vi*) shall have small masses for achieving high minority carrier mobility. In addition to this, the material shall of course, as for regular thin-film PV, (*vii*) involve only earth abundant, non-toxic, and inexpensive elements, and the devices shall be inexpensive regarding fabrication and handling. The material must also be (*viii*) thermodynamic stable with no devastating in-gap defect states, be able to be doped, and to have suitable band alignment at the interfaces.

We thank the Research Council of Norway (project 243642) as well as the Swedish Foundation for Strategic Research for financial support. We acknowledge access to HPC resources Abel at UiO in Norway operated by USIT, and allocation provided through NOTUR, Beskow at KTH operated by PDC, Triolith at LiU operated by NSC, both in Sweden and the allocation was provided through SNIC. We also acknowledge PRACE for awarding access to resource MareNostrum based in Spain at BSC-CNS, access to the DECI resource Archer based in the UK Edinburgh with support from the PRACE aisbl.

## References

1. P. Jackson, R. Wuerz, D. Hariskos, E. Lotter, W. Witte, M. Powalla, Phys. Stat. Sol. RRL **10**, 583 (2016)
2. W. Wang, M.T. Winkler, O. Gunawan, T. Gokmen, T.K. Todorov, Y. Zhu, and D.B. Mitzi, Adv. Energy Mater. **4**, 1301465 (2014)
3. N.S. Lewis, D.G. Nocera, Proc. Natl. Acad. Sci. USA **103**, 15729 (2006)
4. M. Kumar, C. Persson, Energy Procedia **44**, 176 (2014)
5. M. Kumar, C. Persson. J. Renew. Sustain. Energy **5**, 031616 (2013)
6. J. Zhou, G.Q. Bian, Q.Y. Zhu, Y. Zhang, C.Y. Li, J. Dai, J Solid State Chem **182**, 259 (2009)
7. A. Rabhi, M. Kanzari, B. Rezig, Thin Solid Films **517**, 2477 (2009)
8. Y. Rodriguez-lazcano, M.T.S. Nair, P.K. Nair, J. Cryst. Growth **223**, 399 (2001)
9. P.S. Sonawane, P.A. Wani, L.A. Patil, T. Seth, Mater. Chem. Phys. **84**, 221 (2004)
10. J.T.R. Dufton, A. Walsh, P.M. Panchmatia, L.M. Peter, D. Colombara, and M.S. Islam, Phys. Chem. Chem. Phys. **14**, 7229 (2013)
11. D.J. Temple, A.B. Kehoe, J.P. Allen, G.W. Watson, D.O. Scanlon, J. Phys. Chem. C **116**, 7334 (2012)
12. D. Colombara, L.M. Peter, K.D. Rogers, J.D. Painter, S. Roncallo, Thin Solid Films **519**, 7438 (2011)
13. S.H. Pawar, A.J. Pawar, P.N. Bhosale, Bull. Mater. Sci. **8**, 423 (1986)
14. D. Tang, J. Yang, F. Liu, Y. Lai, J. Li, Y. Liu, Electrochim. Acta **76**, 480 (2012)
15. W. Septina, S. Ikeda, Y. Iga, T. Harada, M. Matsumura, Thin Solid Films **550**, 700 (2014)
16. A.W. Welch, L.L. Baranowski, P. Zawadzki, S. Lany, C.A. Wolden, A. Zakutayev, Appl. Phys. Express **8**, 082301 (2015)
17. G. Kresse, D. Joubert, Phys. Rev. B **59**, 1758 (1999)
18. P.E. Blöchl, O. Jepsen, O.K. Andersen, Phys. Rev. B **49**, 16223 (1994)
19. M. Gajdoš, K. Hummer, G. Kresse, J. Furthmüller, F. Bechstedt, Phys. Rev. B **73**, 045112 (2006)
20. J. Heyd, G.E. Scuseria, M. Ernzerhof, J. Chem. Phys. **118**, 8207 (2003)

21. A. Crovetto, R. Chen, R.B. Ettlinger, A.C. Cazzaniga, J. Schou, C. Persson, O. Hansen, Sol. Energy Mater. Sol. Cells **154**, 121 (2016)
22. S. Tomiæ, L. Bernasconi, B.G. Searle, N.M. Harrison, J. Phys. Chem. C **118**, 14478 (2014)
23. C. Persson, S. Mirbt, Br. J. Phys. **36**, 286 (2006)
24. C. Persson, R. Ahuja, B. Johansson, Phys. Rev B **64**, 033201 (2001)
25. W. Shockley, H.J. Queisser, J. Appl. Phys. **32**, 510 (1961)
26. A. Cuevas, Energy Procedia **55**, 53 (2014)
27. K.L. Chopra and S.R. Das, in *Thin Film Solar Cells*, 1st edn. (Springer, New York, 1983)
28. C. Persson, J. Appl. Phys. **107**, 053710 (2010)
29. S. Li, S. Zamulko, C. Persson, N. Ross, J. Larsen, C. Platzer-Björkman, Appl. Phys. Lett. **110**, 021905 (2017)
30. C. Persson, App. Phys. Lett. **93**, 072106 (2008)
31. R. Chen, C. Persson, J. Appl. Phys. **112**, 103708 (2012)
32. S. Dominici, H. Wen, F. Bertazzi, M. Goano, E. Bellotti, Appl. Phys. Lett. **108**, 211103 (2016)
33. D. Steiauf, E. Kioupakis, C.G. Van de Walle, ACS Photonics **108**, 211103 (2006)
34. J. Dziewior, W. Schmid, Appl. Phys. Lett. **31**, 346 (1977)
35. R.A. Sinton, R.M. Swanson, IEEE Trans. Electron Dev. **ED–34**, 1380 (1987)
36. L. Yu, A. Zunger, Phys. Rev. Lett. **108**, 068701 (2012)

**Cite this article as:** Rongzhen Chen, Clas Persson, High absorption coefficients of the $CuSb(Se,Te)_2$ and $CuBi(S,Se)_2$ alloys enable high-efficient 100 nm thin-film photovoltaics , EPJ Photovoltaics **8**, 85504 (2017).